

BBQ-to-Image: Numeric Bounding Box and Qolor Control in Large-Scale Text-to-Image Models

Eliran Kachlon Alexander Visheratin Nimrod Sarid Tal Hacham Eyal Gutflaish
Saar Huberman Hezi Zisman David Ruppin Ron Mokady

BRIA AI



Figure 1: **Bounding-box and RGB-controlled image generation and refinement.** BBQ enables precise spatial and color control by conditioning on explicit numeric bounding boxes and RGB values. In the example, the exact locations of the people and the dog are specified via bounding boxes, and the colors of their clothing are defined using RGB triplets. Beyond initial generation, BBQ enables structured refinement by modifying only the numeric parameters in the caption and re-generating the image. Due to the model’s disentangled control over layout and color, updating bounding boxes (e.g., swapping the man and the woman, or moving the dog to the right) or modifying RGB values results in consistent, targeted changes while preserving the rest of the scene.

Abstract

Text-to-image models have rapidly advanced in realism and controllability, with recent approaches leveraging long, detailed captions to support fine-grained generation. However, a fundamental *parametric gap* remains: existing models rely on descriptive language, whereas professional workflows require precise numeric control over object location, size, and color. In this work, we introduce *BBQ*, a large-scale text-to-image model that directly conditions on numeric bounding boxes and RGB triplets within a unified structured-text framework. We obtain precise spatial and chromatic control by training on captions enriched with parametric annotations, without architectural modifications or inference-time optimization. This also enables intuitive user interfaces such as object dragging and color pickers, replacing ambiguous iterative prompting with precise, familiar controls. Across comprehensive evaluations, *BBQ* achieves strong box alignment and improves RGB color fidelity over state-of-the-art baselines. More broadly, our results support a new paradigm in which user intent is translated into an intermediate structured language, consumed by a flow-based transformer acting as a renderer and naturally accommodating numeric parameters.

1 Introduction

Text-to-image models have rapidly evolved from casual creative tools into professional-grade systems, achieving unprecedented levels of realism and visual fidelity. Recent works have significantly advanced controllability by training on long structured captions, most notably *FIBO* [1], as well as concurrent systems such as Hunyuan 3.0 [2] and FLUX.2 [3]. By encoding fine-grained visual attributes explicitly in text, these models allow users to specify and control nearly every aspect of an image using language alone. Unlike earlier approaches, such models exhibit natural disentanglement, enabling refinement of a specific visual factor, such as lighting, object appearance, or expression, while keeping other aspects unchanged.

Despite this progress, a fundamental *parametric gap* remains. Text-based controllability is inherently descriptive and imprecise for attributes that require exact numeric specification. In this work, we focus on three such attributes: *size*, *location*, and *color*. Current models rely on subjective linguistic descriptors such as “crimson” or “bottom-right,” whereas professional workflows demand deterministic precision in the form of explicit RGB values and pixel-accurate bounding boxes. Moreover, parametric grounding naturally enables intuitive interaction: bounding boxes support direct object manipulation (e.g., dragging), and RGB values integrate seamlessly with

color pickers. This replaces ambiguous natural-language prompting with precise and familiar user interfaces.

In this paper, we show that large-scale text-to-image models can be adapted to process *numeric inputs* for precise parametric control. We introduce *BBQ*, a large-scale text-to-image model capable of controlling Bounding Boxes and Colors directly. Unlike prior approaches, *BBQ* requires no architectural modifications, no special grounding tokens, and no inference-time optimization. Instead, parametric control is achieved solely by augmenting the training captions, resulting in a simple yet powerful solution that scales naturally to professional use.

To generate training data, we augment *FIBO*-style structured captions with explicit numeric attributes, including RGB color values and object bounding boxes. For inference, we fine-tune a vision-language model (VLM) to serve as an inference-time bridge, converting short natural-language prompts into detailed parametric descriptions that *BBQ* can execute faithfully.

More broadly, our framework highlights a new paradigm for image generation. Rather than generating images directly from user-written text, user intent is first translated, by a VLM, into an intermediate, structured language, which is then consumed by a flow-based transformer acting as a renderer. Within this paradigm, we show that the intermediate language can naturally accommodate numeric parameters, enabling precise, deterministic control without sacrificing expressiveness.

Through extensive evaluation, we demonstrate that *BBQ* achieves strong results in precision for object location, size, and color control, demonstrating that large-scale text-to-image models can natively process numeric parameters within a unified text-based framework.

2 Related Works

Text-to-image models. Diffusion models have become the primary framework for text-to-image generation. Early models [4–6] established the power of conditioning on strong language encoders, while latent diffusion made large-scale training practical [7, 8]. Recently, architectures have shifted toward transformer backbones and flow-matching objectives [9–13]. Together, these advances have pushed the boundaries of visual fidelity.

Long and structured captions. While early models relied on noisy, web-scraped data [14], recent works [9, 11, 15] show that descriptive synthetic captions significantly improve prompt alignment. Recently, *FIBO* [1] extended this approach by using vision-language models to produce long, structured JSON captions that capture all visual factors in the image, including object attributes, spatial relations, and photographic style. This ap-

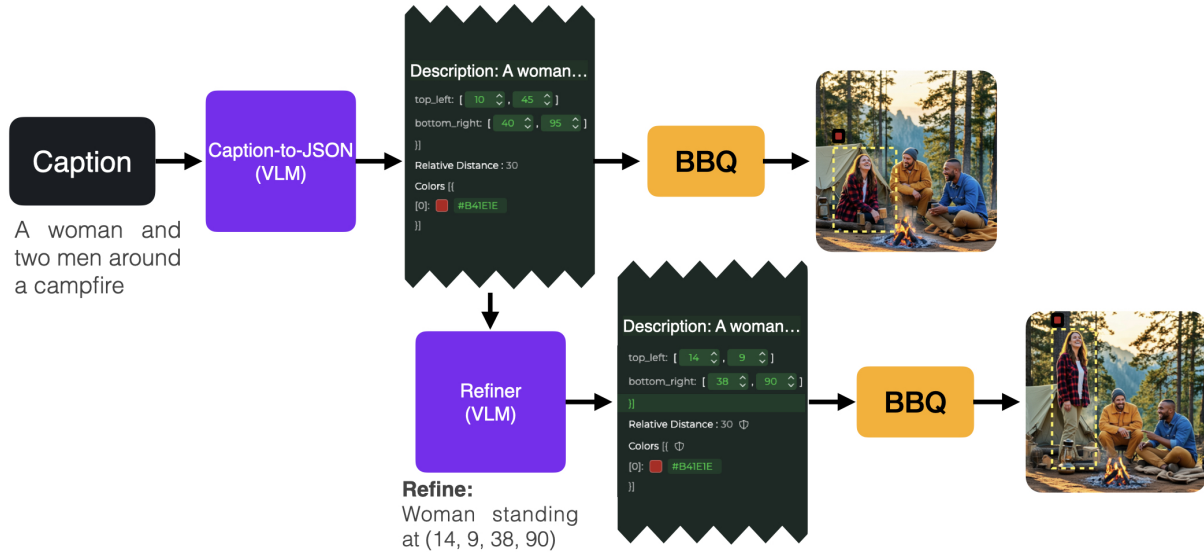


Figure 2: **End-to-end parametric workflow.** A short prompt is expanded by a VLM into a structured JSON that includes numeric bounding boxes and RGB values (for clarity, we show only the parametric fields for the woman). The JSON is then provided to BBQ to generate an image. Users can edit specific fields (e.g., box coordinates or color values), and BBQ updates the output accordingly while preserving unrelated content, demonstrating native disentanglement. Notably, BBQ receives no image input, and consistency is maintained solely through the disentangle structured conditioning.

proach achieved state-of-the-art prompt alignment and introduced fine-grained control, enabling “native disentanglement” where modifying a single attribute in the JSON affects only the intended visual factor. However, FIBO relies on natural language (e.g., “red” or “top-left”) that still involves semantic ambiguity. BBQ builds on this foundation by replacing descriptive strings with absolute precision, integrating RGB values and bounding boxes to transition from semantic alignment to exact pixel-level and chromatic controllability.

Region-controlled text-to-image. Traditional layout-to-image frameworks [7, 16–22] that generate images given bounding boxes are usually limited to constrained vocabularies [23]. Recent works like ReCo [24], GLIGEN [25], InstanceDiffusion [26] and Ranni [27] mitigate these gaps by introducing specialized position tokens or modifying model architectures to inject regional grounding signals. Related controllable diffusion frameworks such as ControlNet [28] and Composer [29] further enable spatial control through additional conditioning pathways. Training-free approaches such as BoxDiff [30] and MultiDiffusion [31] also support region constraints by altering the denoising process at inference time. While effective, these approaches necessitate complex structural changes, auxiliary conditioning mecha-

nisms, or inference-time modifications. In contrast, BBQ unifies high-precision spatial control within a single structured textual representation, enabling exact coordinate guidance without any architectural modifications to the underlying model.

Color-palette generation. Controlling color distribution is a classical challenge in image synthesis [32–36]. Early deep learning efforts incorporated generative and adversarial frameworks to better model realistic and diverse color distributions [37–44]. More recent approaches attempt to provide fine-grained control over color attributes within text-to-image diffusion models. These include methods that train and fine-tune existing models [27, 29, 45], as well as training-free approaches [46–48] that enable color control by manipulating the sampling process or exploiting existing semantic bindings, bypassing the need for additional fine-tuning. However, these methods often rely on specialized adapters, task-specific loss functions, or additional inference-time optimization steps. In contrast, BBQ achieves precise RGB-level color attribution by encoding explicit RGB triplets directly within the textual conditioning, without introducing architectural changes or inference-time modifications.

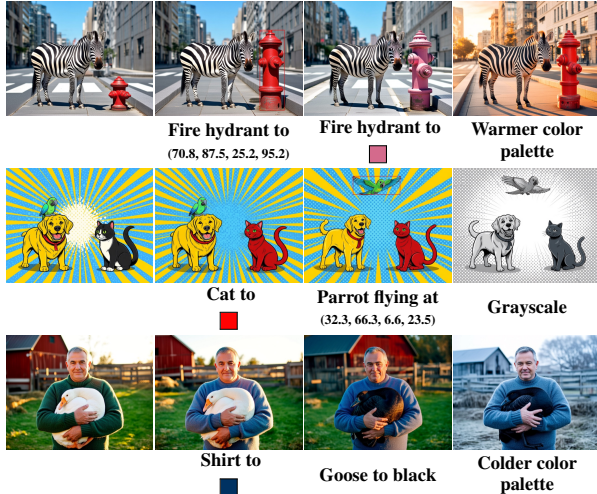


Figure 3: **Disentangled parametric refinement via structured re-generation.** Each example starts from an image generated from a structured JSON prompt. We then edit only the relevant JSON fields and re-generate using the same random seed. Although the model does not observe the original image, it produces localized changes that follow the modified parameters while preserving the rest of the scene, demonstrating strong parametric disentanglement. Ground-truth bounding boxes are overlaid for visualization.

3 Method

We now describe our framework, BBQ. Our objective is to adapt a large-scale text-to-image model to accept *numeric* bounding boxes and colors as conditioning inputs, such that the generated image is faithfully aligned with these parametric specifications.

Formally, let \mathcal{M} denote a text-to-image model trained to generate images conditioned on a long structured caption \mathcal{P} [1]. We extend this model to additionally condition on numeric bounding boxes $\{b_i\}_{i=1}^N$ and colors $\{c_i\}_{i=1}^N$ for each of the N objects in \mathcal{P} , producing an image

$$\mathcal{M}(\mathcal{P}, \{b_i\}_{i=1}^N, \{c_i\}_{i=1}^N)$$

that is accurately aligned with the specified parameters. Unlike standard text-to-image generation, where spatial and chromatic attributes are described linguistically, bounding boxes and colors in our framework are represented numerically: (1) each bounding box is defined as $b = (x_0, y_0, x_1, y_1) \in (0, 1)^4$, where (x_0, y_0) and (x_1, y_1) are the relative coordinates corresponding to the top-left and bottom-right of the bounding box, and (2) each color is defined as an RGB triplet $c \in [0, 255]^3$.

In this section, we show that such adaptation is feasible at large scale *without* architectural changes or additional loss functions, relying solely on dataset aug-



Figure 4: **Text-as-a-Bottleneck Reconstruction (TaBR).** Starting from the original image (left), a detailed caption is generated and used as input to each model. The resulting reconstructions are compared against the original. BBQ more faithfully preserves scene layout, object relations, and fine-grained attributes than competing state-of-the-art models, demonstrating improved expressiveness.

mentation. In Section 3.1, we describe how we augment structured training captions with numeric bounding boxes and colors $(\{b_i\}_{i=1}^N, \{c_i\}_{i=1}^N)$. Section 3.2 details the training procedure of BBQ, including the incorporation of parametric supervision without architectural modifications. Finally, in Section 3.3, we describe how we bridge the gap between user intent and a valid structured prompt. Specifically, we first present the translation of a short natural-language caption into a full long structured parametric prompt $(\mathcal{P}, \{b_i\}_{i=1}^N, \{c_i\}_{i=1}^N)$, and then describe how users can interactively modify bounding boxes or colors, e.g., by dragging objects or adjusting color values, while maintaining global consistency within the structured representation.

3.1 Enriching the Training Data with Bounding Boxes and Colors

In BBQ, we extend the common practice of synthetic captioning for text-to-image training. Starting from long structured captions [1], we augment each caption with *numeric* bounding boxes and RGB colors. Although extracting such parameters is well studied in vision and graphics, we find that general-purpose LLM/VLM systems (e.g., Gemini 2.5 [49]) are not sufficiently reliable for high-precision outputs. Therefore, for each image we first generate a FIBO-style structured caption, following [1]. For every object mentioned in the caption, we extract its bounding box from grounded SAM2 [50], estimate relative depth using Depth Anything V2 [51], and obtain

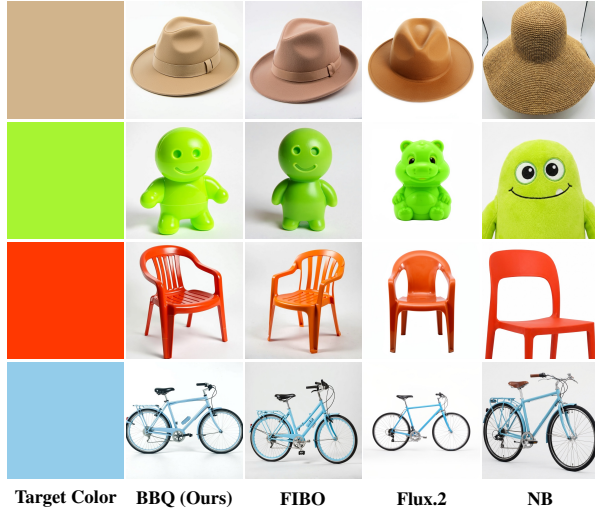


Figure 5: **Color-conditioning accuracy.** Each example shows the target color (left) and images generated by different models when conditioned on the same object and exact RGB value. BBQ achieves high chromatic fidelity to the target color and produces competitive results compared to state-of-the-art text-to-image models under identical color-conditioning prompts.

dominant object colors using Pylette [52]. We replace semantic location and qualitative color terms with explicit bounding box coordinates and RGB triplets. Finally, a global RGB palette from Pylette is added to capture the overall color scheme. This automated extraction provides the precise parametric grounding required to align numeric tokens with visual synthesis.

3.2 BBQ: Large-Scale Training to Control Bounding Boxes and Colors

Unlike prior approaches that introduce new architectures, loss functions, or extended inference procedures to enable parametric control, we show that strong bounding-box grounding can be achieved by large-scale training on enriched captions alone. We initialize from the 8B-parameter FIBO backbone [1], which is designed to process long structured captions, and continue training on 25M images paired with our parametric captions.

We train the model following FIBO’s hyperparameters [1], using the AdamW optimizer [53] with weight decay of 1×10^{-4} , $\beta_1 = 0.9$, $\beta_2 = 0.999$, and $\epsilon = 1 \times 10^{-15}$. The learning rate is set to 1×10^{-4} with a constant schedule and a warmup of 10K steps. Training follows the flow-matching formulation [54], with a logit-normal noise schedule combined with resolution-dependent timestep shifting [9]. The model was trained for 80,000 steps with an effective batch size of 512 in resolution 1024^2 . Post-

“A knight located at (top left: (27.2, 36.3), bottom right: (54.8, 98)) is going towards a dragon at (top left: (63.1, 14.7), bottom right: (77.1, 29.1)).”



“Three glass bottles standing in a row: a red bottle at (top left: (12.5, 30), bottom right: (27.5, 80)), a green bottle at (top left: (42.5, 30.0), bottom right: (57.5, 80.0)), and a blue bottle at (top left: (72.6, 30.0), bottom right: (87.6, 80.0)).”



“A monkey at (“top left”: (16.5, 59.8), “bottom right”: (35, 85)) is going towards a zebra at (“top left”: (54.3, 17.1), “bottom right”: (92.3, 89.7))”

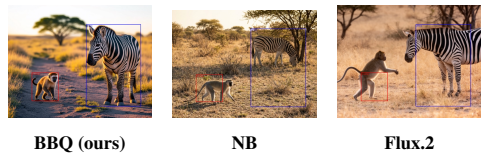


Figure 6: **Bounding-box accuracy.** We compare BBQ with Nano Banana Pro and Flux.2 Pro on prompts that include explicit numeric bounding-box specifications (overlaid on the images). While the baseline models often struggle to consistently follow these spatial constraints, BBQ reliably places objects within the specified boxes.

training, we perform aesthetic finetuning with 3,000 hand-picked images, followed by DPO training [55] with dynamic beta [56] to improve text rendering.

As shown in Figure 1, BBQ adapts effectively to the new conditioning format and follows numeric inputs with high fidelity. Furthermore, Figure 3 demonstrates that BBQ preserves FIBO’s native disentanglement: using the same random seed, we modify only the relevant fields in the structured JSON and re-generate the image, resulting in targeted changes to the specified attribute while the rest of the scene remains largely unchanged.

3.3 The Parametric Bridge: From Short Captions to Long, Structured, Parametric Prompts

The trained model enables new forms of user interaction, including object dragging, resizing, and recoloring. However, building a complete end-to-end system introduces two key challenges. First, when a user edits a bounding box, the system must preserve global coherence and avoid breaking the composition. For example, if two people are hugging and the user separates their boxes, the underlying action must necessarily change. Second, for generation from scratch, a short natural-language prompt must

Table 1: **Text-as-a-Bottleneck Reconstruction (TaBR)**. Win rate is computed as the fraction of images where BBQ is preferred over the competing model among decisive comparisons (ties ignored). Confidence intervals correspond to 95% Wilson score intervals. BBQ outperforms all evaluated baselines across all comparisons.

Model (vs. BBQ)	BBQ win rate \uparrow	95% CI
Nano Banana Pro	65.2%	[50.8, 77.3]
FIBO	76.1%	[62.1, 86.1]
FLUX.2 Pro	93.3%	[82.1, 97.7]

be expanded into a full structured caption with a plausible composition, now including explicit bounding boxes and colors. While BBQ provides unprecedented precision through its parametric schema, manually authoring JSON prompts with exact RGB triplets and normalized bounding box coordinates is impractical for human users.

To address these inference-time gaps, we fine-tune Qwen-3 VL 4B [57] to serve as an inference-time *bridge* that translates natural-language intent into the parametric language consumed by the generator. We train on synthetically generated short prompts and editing instructions, using the same structured schema employed for FIBO BBQ. Training is performed on $8\times H100$ with a total of 3B tokens. To improve robustness, we decouple image-conditioned and text-only tasks during training and repeat each with different seeds, then final weights are produced via model merging [58].

The VLM operates in three modes: (1) *Generate*, which expands a brief prompt into a complete parametric JSON; (2) *Refine*, which edits an existing JSON in response to textual instructions (e.g., shifting bounding boxes or adjusting colors) while maintaining internal consistency; and (3) *Inspire*, which extracts a parametric description from a reference image to serve as a template for generation and editing. In practice, we find that state-of-the-art VLMs such as Gemini 2.5 [49] can also serve as an effective inference-time bridge. The workflow of BBQ is described in Figure 2.

4 Experiments

In this section, we present a comprehensive evaluation of BBQ, comparing it to existing state-of-the-art models. Our experiments are designed to isolate three complementary properties: (1) expressiveness, (2) spatial accuracy under numeric box constraints, and (3) color fidelity under explicit RGB specification. Evaluation methods are described in Section 4.1, qualitative results are provided in Section 4.2, and quantitative results are discussed in Section 4.3.

4.1 Evaluation Metrics

We evaluate BBQ using three complementary metrics that capture different aspects of controlled image synthesis: (1) *Text-as-a-Bottleneck Reconstruction (TaBR)* [1] measures overall expressiveness via caption \rightarrow generation \rightarrow reconstruction, (2) *Bounding-box accuracy* measures spatial grounding under box-conditioned prompts, using COCO with YOLO-based detection [23, 59] and LVIS with box-conditioned zero-shot grounding [60], and (3) *Color accuracy* measures parametric color fidelity by clustering generated pixels in CIELab space using K-means and reporting perceptual color differences via CIEDE2000 (ΔE_{00}) and the *a-b* chroma distance. For TaBR and color accuracy, we compare BBQ against state-of-the-art text-to-image baselines (FIBO, Nano Banana Pro, and Flux.2 Pro). For bounding-box accuracy, we additionally compare against InstanceDiffusion [26] and GLIGEN [25], widely used box-grounded generation methods.

Text-as-a-Bottleneck. TaBR [1] measures the overall expressive power by anchoring the evaluation in images rather than subjective text reasoning. Following FIBO, we begin with a real image, produce a detailed caption using a VLM, and then regenerate the image from this caption alone. Annotators are then presented with the original image alongside two reconstructions from different models and asked: “Which image is more similar to the original?” Like in FIBO, we perform this measurement on a test-set of 60 image that are not part of our training data.

For BBQ and FIBO we utilize their native structured schemas for compatibility, while for Nano Banana Pro and Flux.2 Pro, we report the best result among three methods: (a) BBQ parametric captions, (b) FIBO long structured captions, and (c) detailed free-text descriptions including precise Hex codes for object colors. To avoid evaluation bias from the captioning pipeline, we use a *neutral* VLM that is independent of BBQ and the data preparation used for FIBO.

YOLO- and LVIS-based scores. We follow the evaluation protocol of InstanceDiffusion [26] to assess spatial alignment between generated images and input bounding boxes. A pretrained object detector is applied to the generated images, and the predicted boxes are compared against the input box coordinates. For COCO evaluation, we use YOLOv8 and report AP , AP_{50} , and AR on COCO2017-val. For large-vocabulary evaluation, we follow the LVIS protocol using a ViTDet-L detector.

Color-conditioning accuracy. To evaluating color fidelity we wish to isolate the specific object and remove

Table 2: **Bounding-box alignment under box-conditioned generation on COCO and LVIS.** We follow the InstanceDiffusion evaluation protocol using YOLO-based detection; the upper bound corresponds to detector performance on real images. Across both datasets, BBQ consistently outperforms strong text-to-image baselines (Nano Banana Pro and Flux.2 Pro) and GLIGEN, while trailing the specialized InstanceDiffusion approach. Importantly, BBQ achieves this without architectural modifications or grounding-specific components and is trained for high-fidelity image synthesis, providing strong spatial control within a general large-scale and disentangle model, also allowing intuitive refinement. Best results are in **bold**; second best are underlined.

Method	COCO			LVIS							
	AP	AP ₅₀	AR	AP	AP ₅₀	AP _s	AP _m	AP _l	AP _r	AP _c	AP _f
Upper bound (real images)	50.2	66.7	61.0	44.6	57.7	33.2	55.0	66.1	31.4	44.5	50.5
Flux.2 Pro	3.5	8.7	4.6	2.1	4.8	0.1	0.8	7.3	0.1	0.2	2.4
Nano Banana Pro	5	11.3	5.5	4.1	10.6	0.1	1	15.9	3.3	4	3.9
GLIGEN [25]	19.6	35.0	30.7	9.9	9.5	<u>1.6</u>	10.5	31.1	7.4	10.0	10.9
BBQ (ours)	<u>28.6</u>	<u>40.9</u>	<u>38.2</u>	<u>13.1</u>	<u>20.1</u>	<u>1.6</u>	13.9	<u>37.4</u>	13.1	<u>14.0</u>	<u>12.7</u>
InstanceDiffusion [26]	38.8	55.4	52.9	17.9	25.5	5.5	24.2	45.0	<u>12.7</u>	18.7	19.3

Table 3: **Color fidelity comparison.** ΔE_{00} (CIEDE2000) measures perceptual color difference, while $a-b$ distance captures chromaticity (hue and saturation) independently of lightness. We report mean, median, and 90th percentile (p90), where lower values indicate better color accuracy.. Across both $K = 5$ and $K = 8$, BBQ achieves the lowest $a-b$ errors in all statistics, indicating the most accurate chromaticity control and fewer severe failures, while remaining competitive under ΔE_{00} that penalizes lightness differences. Best results are in **bold** and second-best are underlined (computed per K).

K	Model	$a-b$ Mean \downarrow	$a-b$ Median \downarrow	$a-b$ p90 \downarrow	ΔE_{00} Mean \downarrow	ΔE_{00} Median \downarrow	ΔE_{00} p90 \downarrow
5	BBQ (ours)	7.16	6.67	13.30	5.93	<u>5.76</u>	9.62
	Nano Banana Pro	10.91	<u>7.52</u>	20.80	<u>6.50</u>	5.72	11.00
	FLUX.2 Pro	<u>10.07</u>	8.16	<u>19.30</u>	6.64	6.12	<u>10.17</u>
	FIBO	10.32	9.44	20.36	6.74	7.32	10.52
8	BBQ (ours)	7.48	6.23	14.33	<u>5.74</u>	<u>5.07</u>	9.89
	Nano Banana Pro	10.64	<u>6.87</u>	21.05	5.91	4.82	10.80
	FLUX.2 Pro	<u>9.50</u>	8.26	<u>17.98</u>	5.67	5.42	<u>9.99</u>
	FIBO	11.07	9.62	20.52	6.99	5.90	11.03

noise from other parts of the image. Therefore, we generated 200 images depicting single objects on white background, where each object was assigned a specific target RGB color in the prompt. For evaluation, we extract object pixels by masking out the white background using foreground segmentation, and then apply K-means clustering (with $K = 5$ and $K = 8$) in CIELab color space on the extracted object pixels to identify the dominant color palette. Clusters representing less than 5% of object pixels are filtered out. Among the remaining clusters, we select the one with the minimum distance to the target color. We report two distance metrics: ΔE_{00} (CIEDE2000), which measures perceptual color difference, and Euclidean distance in the $a-b$ chromaticity plane, which isolates hue and saturation differences independently of light. For both metrics, we report mean, median, and 90th percentile (p90) statistics, where p90 captures tail behavior and robustness to difficult cases that may not be reflected by central tendency alone. Like in TaBR, BBQ and FIBO

utilize their native structured schemas for compatibility, where for FIBO we ask the VLM to choose the name of the color that best describes the RGB. For Flux.2 Pro we follow the prompting guide [61] and for Nano Banana Pro we’ve found that the best results are achieved with the same prompts as Flux.

4.2 Qualitative Results

In Figure 4, we present TaBR reconstructions, where BBQ faithfully preserves the original pose, object relationships, and overall scene layout. Figure 5 illustrates BBQ’s ability to follow explicit numeric color specifications: when conditioned on exact RGB values, the model produces visually accurate object colors and remains competitive with state-of-the-art baselines. Figure 6 provides qualitative comparisons for bounding-box grounding against strong general-purpose models, Nano Banana Pro and Flux.2 Pro. While these baselines often struggle to sat-

isfy explicit numeric box constraints, BBQ consistently aligns object placement with the specified regions, motivating our subsequent quantitative comparison against dedicated layout-aware approaches such as InstanceDiffusion and GLIGEN. Additional results are presented in Figure 7 demonstrating the effectiveness of our approach.

4.3 Quantitative Results

Text-as-a-Bottleneck. Table 1 reports image-level pairwise preference results for the TaBR evaluation. We report the win rate of BBQ as the fraction of images where it is preferred over the competing model among decisive outcomes (ties ignored), together with 95% Wilson score confidence intervals. As shown in the table, BBQ consistently outperforms its predecessor FIBO as well as state-of-the-art general-purpose text-to-image models, including Nano Banana Pro and Flux.2 Pro, demonstrating that incorporating explicit numeric parameters improves reconstruction fidelity without sacrificing global coherence.

Bounding-box accuracy. Table 2 evaluates spatial grounding under box-conditioned prompts on COCO and LVIS. Across both datasets, BBQ consistently outperforms strong text-to-image baselines such as Nano Banana Pro and Flux.2 Pro, as well as the dedicated grounding model GLIGEN, while trailing the current state-of-the-art InstanceDiffusion. These results position BBQ as a strong non-specialized alternative for box-conditioned generation. Unlike InstanceDiffusion and GLIGEN, which rely on grounding-specific architectural modifications or inference-time alignment mechanisms, BBQ is trained at a substantially larger scale for general high-fidelity image synthesis, achieving strong bounding-box alignment without sacrificing expressiveness, inference time or requiring specialized components. Furthermore, unlike InstanceDiffusion, BBQ exhibits native disentanglement that enables intuitive parametric refinement, as illustrated in Fig. 7 and Fig. 3

Color-conditioning accuracy. Table 3 reports color fidelity using two complementary metrics. We primarily focus on Euclidean distance in the a–b chromaticity plane, which isolates hue and saturation differences while ignoring lighting, making it better aligned with our goal of precise parametric color control independent of illumination and shading. Under this metric, BBQ consistently outperforms all competing models for both $K = 5$ and $K = 8$, achieving the lowest mean, median, and 90th-percentile errors, and indicating both superior average accuracy and substantially fewer severe failures. We also report CIEDE2000 (ΔE_{00}), which penalizes lightness variation; some baselines achieve lower scores via

more uniform lighting, whereas BBQ preserves accurate chromaticity under realistic lighting.

5 Conclusion

In this work, we introduced BBQ, a large-scale text-to-image model that enables precise control over object location, size, and color, through explicit numeric bounding boxes and RGB values. BBQ directly addresses the parametric gap between descriptive language and the deterministic numeric control required in professional workflows, demonstrating that such precision can be achieved purely through large-scale training on enriched structured captions, without architectural modifications or inference-time optimization. More broadly, BBQ highlights the power of structured intermediate representations as a bridge between user intent and generative rendering. By translating natural-language prompts into a parametric schema that supports direct numeric manipulation, our framework enables intuitive interactive interfaces, such as object repositioning and precise color selection, while maintaining global scene coherence. This approach suggests a path toward programmable, professional-grade image synthesis systems that integrate additional precise attributes, moving beyond descriptive prompting toward truly controllable generative modeling.

References

- [1] Eyal Gutflaish, Eliran Kachlon, Hezi Zisman, Tal Hacham, Nimrod Sarid, Alexander Visheratin, Saar Huberman, Gal Davidi, Guy Bukchin, Kfir Goldberg, et al. Generating an image from 1,000 words: Enhancing text-to-image with structured captions. *arXiv preprint arXiv:2511.06876*, 2025.
- [2] Siyu Cao, Hangting Chen, Peng Chen, Yiji Cheng, Yutao Cui, Xincheng Deng, Ying Dong, Kipper Gong, Tianpeng Gu, Xiuse Gu, et al. Hunyuanimage 3.0 technical report. *arXiv preprint arXiv:2509.23951*, 2025.
- [3] Stephen Batifol, Andreas Blattmann, Frederic Boesel, Saksham Consul, Cyril Diagne, Tim Dockhorn, Jack English, Zion English, Patrick Esser, Sumith Kulal, et al. Flux. 1 kontext: Flow matching for in-context image generation and editing in latent space. *arXiv e-prints*, pages arXiv–2506, 2025.
- [4] Alex Nichol, Prafulla Dhariwal, Aditya Ramesh, Pranav Shyam, Pamela Mishkin, Bob McGrew, Ilya Sutskever, and Mark Chen. Glide: Towards photorealistic image generation and editing with text-guided

- diffusion models. *arXiv preprint arXiv:2112.10741*, 2021.
- [5] Chitwan Saharia, William Chan, Saurabh Saxena, Lala Li, Jay Whang, Emily L Denton, Kamyar Ghasemipour, Raphael Gontijo Lopes, Burcu Karagol Ayan, Tim Salimans, et al. Photorealistic text-to-image diffusion models with deep language understanding. *Advances in neural information processing systems*, 35:36479–36494, 2022.
- [6] Aditya Ramesh, Prafulla Dhariwal, Alex Nichol, Casey Chu, and Mark Chen. Hierarchical text-conditional image generation with clip latents. *arXiv preprint arXiv:2204.06125*, 1(2):3, 2022.
- [7] Robin Rombach, Andreas Blattmann, Dominik Lorenz, Patrick Esser, and Björn Ommer. High-resolution image synthesis with latent diffusion models. In *Proceedings of the IEEE/CVF conference on computer vision and pattern recognition*, pages 10684–10695, 2022.
- [8] Dustin Podell, Zion English, Kyle Lacey, Andreas Blattmann, Tim Dockhorn, Jonas Müller, Joe Penna, and Robin Rombach. Sdxl: Improving latent diffusion models for high-resolution image synthesis. *arXiv preprint arXiv:2307.01952*, 2023.
- [9] Patrick Esser, Sumith Kulal, Andreas Blattmann, Rahim Entezari, Jonas Müller, Harry Saini, Yam Levi, Dominik Lorenz, Axel Sauer, Frederic Boesel, et al. Scaling rectified flow transformers for high-resolution image synthesis. In *Forty-first international conference on machine learning*, 2024.
- [10] Black Forest Labs. Flux. <https://github.com/black-forest-labs/flux>, 2024.
- [11] Bingchen Liu, Ehsan Akhgari, Alexander Visheratin, Aleks Kamko, Linmiao Xu, Shivam Shrirao, Chase Lambert, Joao Souza, Suhail Doshi, and Daiqing Li. Playground v3: Improving text-to-image alignment with deep-fusion large language models. *arXiv preprint arXiv:2409.10695*, 2024.
- [12] Qi Cai, Jingwen Chen, Yang Chen, Yehao Li, Fuchen Long, Yingwei Pan, Zhaofan Qiu, Yiheng Zhang, Fengbin Gao, Peihan Xu, et al. Hidream-1l: A high-efficient image generative foundation model with sparse diffusion transformer. *arXiv preprint arXiv:2505.22705*, 2025.
- [13] Chenfei Wu, Jiahao Li, Jingren Zhou, Junyang Lin, Kaiyuan Gao, Kun Yan, Sheng ming Yin, Shuai Bai, Xiao Xu, Yilei Chen, Yuxiang Chen, Zecheng Tang, Zekai Zhang, Zhengyi Wang, An Yang, Bowen Yu, Chen Cheng, Dayiheng Liu, Deqing Li, Hang Zhang, Hao Meng, Hu Wei, Jingyuan Ni, Kai Chen, Kuan Cao, Liang Peng, Lin Qu, Minggang Wu, Peng Wang, Shuting Yu, Tingkun Wen, Wensen Feng, Xiaoxiao Xu, Yi Wang, Yichang Zhang, Yongqiang Zhu, Yujia Wu, Yuxuan Cai, and Zenan Liu. Qwen-image technical report, 2025. URL <https://arxiv.org/abs/2508.02324>.
- [14] Christoph Schuhmann, Romain Beaumont, Richard Vencu, Cade Gordon, Ross Wightman, Mehdi Cherti, Theo Coombes, Aarush Katta, Clayton Mullis, Mitchell Wortsman, et al. Laion-5b: An open large-scale dataset for training next generation image-text models. *Advances in neural information processing systems*, 35:25278–25294, 2022.
- [15] James Betker, Gabriel Goh, Li Jing, Tim Brooks, Jianfeng Wang, Linjie Li, Long Ouyang, Juntang Zhuang, Joyce Lee, Yufei Guo, et al. Improving image generation with better captions. *Computer Science*. <https://cdn.openai.com/papers/dall-e-3.pdf>, 2(3):8, 2023.
- [16] Bo Zhao, Lili Meng, Weidong Yin, and Leonid Sigal. Image generation from layout. In *Proceedings of the IEEE/CVF conference on computer vision and pattern recognition*, pages 8584–8593, 2019.
- [17] Wei Sun and Tianfu Wu. Image synthesis from reconfigurable layout and style. In *Proceedings of the IEEE/CVF International Conference on Computer Vision*, pages 10531–10540, 2019.
- [18] Yandong Li, Yu Cheng, Zhe Gan, Licheng Yu, Liqiang Wang, and Jingjing Liu. Bachgan: High-resolution image synthesis from salient object layout. In *Proceedings of the IEEE/CVF conference on computer vision and pattern recognition*, pages 8365–8374, 2020.
- [19] Stanislav Frolov, Avneesh Sharma, Jörn Hees, Tushar Karayil, Federico Raue, and Andreas Dengel. Attrlostgan: Attribute controlled image synthesis from reconfigurable layout and style. In *DAGM German Conference on Pattern Recognition*, pages 361–375. Springer, 2021.
- [20] Zejian Li, Jingyu Wu, Immanuel Koh, Yongchuan Tang, and Lingyun Sun. Image synthesis from layout with locality-aware mask adaption. In *Proceedings of the IEEE/CVF International Conference on Computer Vision*, pages 13819–13828, 2021.
- [21] Zuopeng Yang, Daqing Liu, Chaoyue Wang, Jie Yang, and Dacheng Tao. Modeling image composition for complex scene generation. In *Proceedings of*

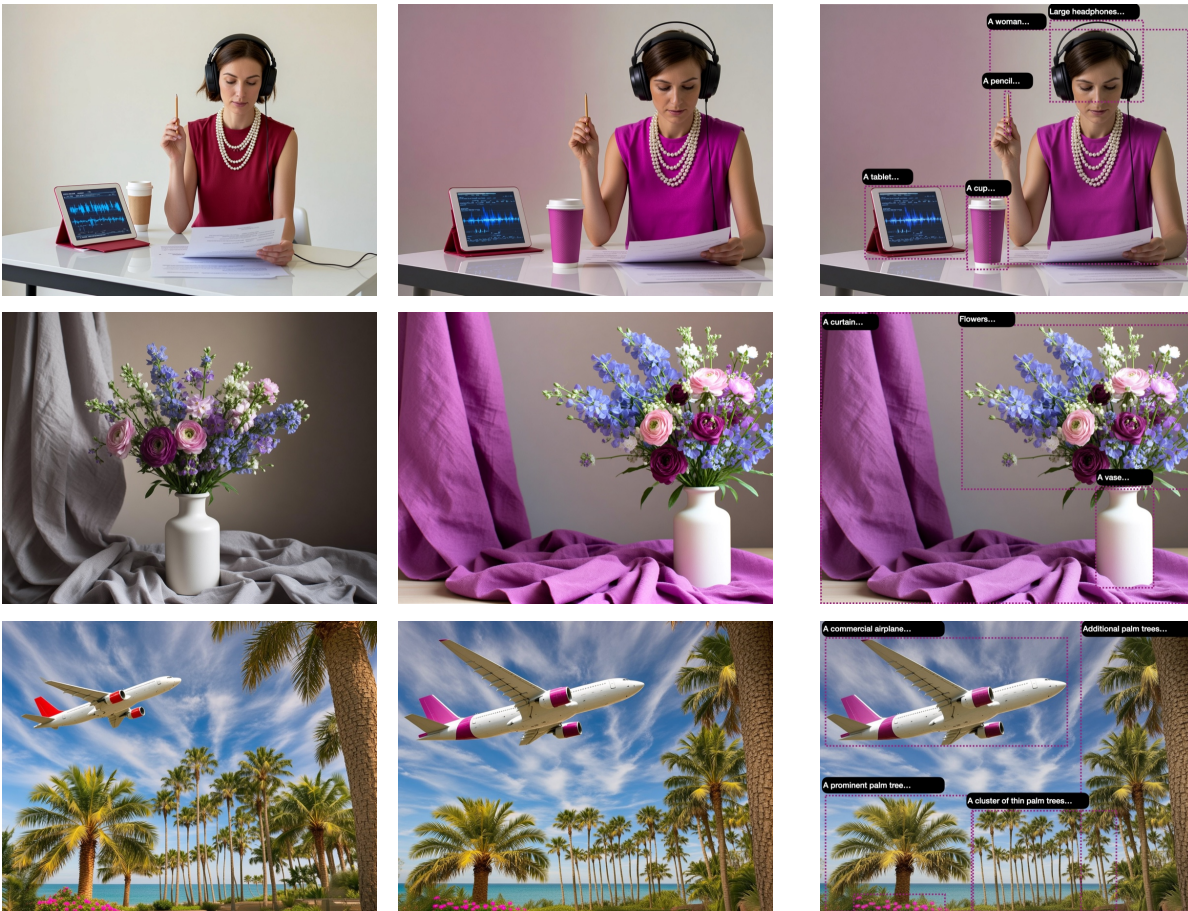
- the IEEE/CVF Conference on Computer Vision and Pattern Recognition*, pages 7764–7773, 2022.
- [22] Wan-Cyuan Fan, Yen-Chun Chen, DongDong Chen, Yu Cheng, Lu Yuan, and Yu-Chiang Frank Wang. Frido: Feature pyramid diffusion for complex scene image synthesis. In *Proceedings of the AAAI conference on artificial intelligence*, volume 37, pages 579–587, 2023.
- [23] Tsung-Yi Lin, Michael Maire, Serge Belongie, James Hays, Pietro Perona, Deva Ramanan, Piotr Dollár, and C Lawrence Zitnick. Microsoft coco: Common objects in context. In *European conference on computer vision*, pages 740–755. Springer, 2014.
- [24] Zhengyuan Yang, Jianfeng Wang, Zhe Gan, Linjie Li, Kevin Lin, Chenfei Wu, Nan Duan, Zicheng Liu, Ce Liu, Michael Zeng, et al. Reco: Region-controlled text-to-image generation. In *Proceedings of the IEEE/CVF Conference on Computer Vision and Pattern Recognition*, pages 14246–14255, 2023.
- [25] Yuheng Li, Haotian Liu, Qingyang Wu, Fangzhou Mu, Jianwei Yang, Jianfeng Gao, Chunyuan Li, and Yong Jae Lee. Gligen: Open-set grounded text-to-image generation. In *Proceedings of the IEEE/CVF conference on computer vision and pattern recognition*, pages 22511–22521, 2023.
- [26] Xudong Wang, Trevor Darrell, Sai Saketh Rambhatla, Rohit Girdhar, and Ishan Misra. Instancediffusion: Instance-level control for image generation. In *Proceedings of the IEEE/CVF conference on computer vision and pattern recognition*, pages 6232–6242, 2024.
- [27] Yutong Feng, Biao Gong, Di Chen, Yujun Shen, Yu Liu, and Jingren Zhou. Ranni: Taming text-to-image diffusion for accurate instruction following. In *Proceedings of the IEEE/CVF Conference on Computer Vision and Pattern Recognition*, pages 4744–4753, 2024.
- [28] Lvmin Zhang, Anyi Rao, and Maneesh Agrawala. Adding conditional control to text-to-image diffusion models. In *Proceedings of the IEEE/CVF International Conference on Computer Vision (ICCV)*, pages 3836–3847, 2023.
- [29] Lianghai Huang, Di Chen, Yu Liu, Yujun Shen, Deli Zhao, and Jingren Zhou. Composer: Creative and controllable image synthesis with composable conditions. In *Proceedings of the 40th International Conference on Machine Learning (ICML)*, pages 13753–13773, 2023.
- [30] Jinheng Xie, Yuexiang Li, Yawen Huang, Haozhe Liu, Wentian Zhang, Yefeng Zheng, and Mike Zheng Shou. Boxdiff: Text-to-image synthesis with training-free box-constrained diffusion. In *Proceedings of the IEEE/CVF International Conference on Computer Vision*, pages 7452–7461, 2023.
- [31] Omer Bar-Tal, Lior Yariv, Yaron Lipman, and Tali Dekel. Multidiffusion: Fusing diffusion paths for controlled image generation. In *Proceedings of the 40th International Conference on Machine Learning (ICML)*, pages 1737–1752, 2023.
- [32] Erik Reinhard, Michael Adhikhmin, Bruce Gooch, and Peter Shirley. Color transfer between images. *IEEE Computer graphics and applications*, 21(5): 34–41, 2002.
- [33] Tomihisa Welsh, Michael Ashikhmin, and Klaus Mueller. Transferring color to greyscale images. In *Proceedings of the 29th annual conference on Computer graphics and interactive techniques*, pages 277–280, 2002.
- [34] Anat Levin, Dani Lischinski, and Yair Weiss. Colorization using optimization. In *ACM SIGGRAPH 2004 Papers*, pages 689–694. 2004.
- [35] Huiwen Chang, Ohad Fried, Yiming Liu, Stephen DiVerdi, and Adam Finkelstein. Palette-based photo recoloring. *ACM Trans. Graph.*, 34(4):139–1, 2015.
- [36] Elad Aharoni-Mack, Yakov Shambik, and Dani Lischinski. Pigment-based recoloring of watercolor paintings. In *Proceedings of the Symposium on Non-Photorealistic Animation and Rendering*, pages 1–11, 2017.
- [37] Richard Zhang, Phillip Isola, and Alexei A Efros. Colorful image colorization. In *European conference on computer vision*, pages 649–666. Springer, 2016.
- [38] Richard Zhang, Jun-Yan Zhu, Phillip Isola, Xinyang Geng, Angela S Lin, Tianhe Yu, and Alexei A Efros. Real-time user-guided image colorization with learned deep priors. *arXiv preprint arXiv:1705.02999*, 2017.
- [39] Chenyang Lei and Qifeng Chen. Fully automatic video colorization with self-regularization and diversity. In *Proceedings of the IEEE/CVF conference on computer vision and pattern recognition*, pages 3753–3761, 2019.

- [40] Jheng-Wei Su, Hung-Kuo Chu, and Jia-Bin Huang. Instance-aware image colorization. In *Proceedings of the IEEE/CVF conference on computer vision and pattern recognition*, pages 7968–7977, 2020.
- [41] Yanze Wu, Xintao Wang, Yu Li, Honglun Zhang, Xun Zhao, and Ying Shan. Towards vivid and diverse image colorization with generative color prior. In *Proceedings of the IEEE/CVF international conference on computer vision*, pages 14377–14386, 2021.
- [42] Satoshi Iizuka, Edgar Simo-Serra, and Hiroshi Ishikawa. Let there be color! joint end-to-end learning of global and local image priors for automatic image colorization with simultaneous classification. *ACM Transactions on Graphics (ToG)*, 35(4):1–11, 2016.
- [43] Hyojin Bahng, Seungjoo Yoo, Wonwoong Cho, David Keetae Park, Ziming Wu, Xiaojuan Ma, and Jaegul Choo. Coloring with words: Guiding image colorization through text-based palette generation. In *Proceedings of the european conference on computer vision (eccv)*, pages 431–447, 2018.
- [44] Yi Wang, Menghan Xia, Lu Qi, Jing Shao, and Yu Qiao. Palgan: Image colorization with palette generative adversarial networks. In *European Conference on Computer Vision*, pages 271–288. Springer, 2022.
- [45] Muhammad Atif Butt, Kai Wang, Javier Vazquez-Corral, and Joost van de Weijer. Colorpeel: Color prompt learning with diffusion models via color and shape disentanglement. In *European Conference on Computer Vision*, pages 456–472. Springer, 2024.
- [46] Alexander Lobashev, Maria Larchenko, and Dmitry Guskov. Color conditional generation with sliced wasserstein guidance. *arXiv preprint arXiv:2503.19034*, 2025.
- [47] Tripti Shukla, Srikrishna Karanam, and Balaji Vasanth Srinivasan. Test-time conditional text-to-image synthesis using diffusion models. *arXiv preprint arXiv:2411.10800*, 2024.
- [48] Héctor Laria, Alexandra Gomez-Villa, Jiang Qin, Muhammad Atif Butt, Bogdan Raducanu, Javier Vazquez-Corral, Joost van de Weijer, and Kai Wang. Leveraging semantic attribute binding for free-lunch color control in diffusion models. *arXiv preprint arXiv:2503.09864*, 2025.
- [49] Gheorghe Comanici, Eric Bieber, Mike Schaekermann, Ice Pasupat, Noveen Sachdeva, Inderjit Dhillon, Marcel Blistein, Ori Ram, Dan Zhang, Evan Rosen, et al. Gemini 2.5: Pushing the frontier with advanced reasoning, multimodality, long context, and next generation agentic capabilities. *arXiv preprint arXiv:2507.06261*, 2025.
- [50] Nikhila Ravi, Valentin Gabeur, Yuan-Ting Hu, Ronghang Hu, Chaitanya Ryali, Tengyu Ma, Haitham Khedr, Roman Rädle, Chloe Rolland, Laura Gustafson, Eric Mintun, Junting Pan, Kalyan Vasudev Alwala, Nicolas Carion, Chao-Yuan Wu, Ross Girshick, Piotr Dollár, and Christoph Feichtenhofer. Sam 2: Segment anything in images and videos. *arXiv preprint arXiv:2408.00714*, 2024. URL <https://arxiv.org/abs/2408.00714>.
- [51] Lihe Yang, Bingyi Kang, Zilong Huang, Zhen Zhao, Xiaogang Xu, Jiashi Feng, and Hengshuang Zhao. Depth anything v2. *arXiv:2406.09414*, 2024.
- [52] qTipTip. Pylette, 2025. URL <https://qtipTip.github.io/Pylette/>.
- [53] Ilya Loshchilov and Frank Hutter. Decoupled weight decay regularization. *arXiv preprint arXiv:1711.05101*, 2017.
- [54] Yaron Lipman, Ricky T. Q. Chen, Heli Ben-Hamu, Maximilian Nickel, and Matt Le. Flow matching for generative modeling, 2023.
- [55] Bram Wallace, Meihua Dang, Rafael Rafailov, Linqi Zhou, Aaron Lou, Senthil Purushwalkam, Stefano Ermon, Caiming Xiong, Shafiq Joty, and Nikhil Naik. Diffusion model alignment using direct preference optimization. In *Proceedings of the IEEE/CVF Conference on Computer Vision and Pattern Recognition*, pages 8228–8238, 2024.
- [56] Jie Liu, Gongye Liu, Jiajun Liang, Ziyang Yuan, Xiaokun Liu, Mingwu Zheng, Xiele Wu, Qiulin Wang, Wenyu Qin, Menghan Xia, et al. Improving video generation with human feedback. *arXiv preprint arXiv:2501.13918*, 2025.
- [57] Shuai Bai, Yuxuan Cai, Ruizhe Chen, Keqin Chen, Xionghui Chen, Zesen Cheng, Lianghao Deng, Wei Ding, Chang Gao, Chunjiang Ge, Wenbin Ge, Zhifang Guo, Qidong Huang, Jie Huang, Fei Huang, Binyuan Hui, Shutong Jiang, Zhaohai Li, Mingsheng Li, Mei Li, Kaixin Li, Zicheng Lin, Junyang Lin, Xuejing Liu, Jiawei Liu, Chenglong Liu, Yang Liu, Dayiheng Liu, Shixuan Liu, Dunjie Lu, Ruilin Luo, Chenxu Lv, Rui Men, Lingchen Meng, Xuancheng Ren, Xingzhang Ren, Sibao Song, Yuchong Sun, Jun Tang, Jianhong Tu, Jianqiang Wan, Peng

Wang, Pengfei Wang, Qiuyue Wang, Yuxuan Wang, Tianbao Xie, Yiheng Xu, Haiyang Xu, Jin Xu, Zhibo Yang, Mingkun Yang, Jianxin Yang, An Yang, Bowen Yu, Fei Zhang, Hang Zhang, Xi Zhang, Bo Zheng, Humen Zhong, Jingren Zhou, Fan Zhou, Jing Zhou, Yuanzhi Zhu, and Ke Zhu. Qwen3-vl technical report. *arXiv preprint arXiv:2511.21631*, 2025.

- [58] Enneng Yang, Li Shen, Guibing Guo, Xingwei Wang, Xiaochun Cao, Jie Zhang, and Dacheng Tao. Model merging in llms, mllms, and beyond: Methods, theories, applications and opportunities. *arXiv preprint arXiv:2408.07666*, 2024.
- [59] Glenn Jocher, Jing Qiu, and Ayush Chaurasia. Ultralytics YOLO, January 2023. URL <https://github.com/ultralytics/ultralytics>.
- [60] Agrim Gupta, Piotr Dollar, and Ross Girshick. Lvis: A dataset for large vocabulary instance segmentation. In *Proceedings of the IEEE/CVF conference on computer vision and pattern recognition*, pages 5356–5364, 2019.
- [61] Black Forest Labs. Prompting guide – flux.2 [pro] & [max], 2025. URL https://docs.bfl.ai/guides/prompting_guide_flux2. Accessed: 2026-02-02.

A Additional Refinement Examples



Original

Refined

Refined with overlaid bounding boxes

Figure 7: **Refinement via structured parametric editing.** The left column shows the original generations, while the middle column presents refined results obtained by editing the structured parametric caption and re-generating the image. In each example, both the numeric bounding boxes (object position and extent) and the object color are modified, explicitly enforcing the target color `#DD20A7`, resulting in updated spatial layout and appearance while preserving overall scene coherence. The right column overlays the exact numeric bounding boxes on the refined images, illustrating precise alignment with the edited parameters.